# Chapter 3

# Statistical Analysis

Scientific investigations generally start with a hypothesis, which is then tested against empirical data. This chapter focuses on the frequentist statistical methods used to evaluate whether the observed collision data support or contradict the proposed hypothesis.

Central to this discussion is the concept of the p-value, which arises within hypothesis testing. The p-value quantifies the compatibility of the observation with the assumption and is particularly important in High Energy Physics (HEP), to confidently determine if a hypothesized process is realized in nature.

Specifically for this task in HEP, the HISTFACTORY framework has been developed. This section the fundamentals of the approach and its implementation [30, 31]. The following is based on [30, 32, 33].

## 3.1 Profile Likelihood Ratio

The statistical model needs to reflect the compatibility of predictions with the observed collision events. This can be quantified by a likelihood function $L(\boldsymbol{x}|\boldsymbol{\phi})$ which can be understood as a probability measure for an observation $\boldsymbol{x}$ under a given set of parameters $\boldsymbol{\phi}$. In this counting experiment, histograms are the primary tool of analysis.

The set of parameters $\boldsymbol{\phi}$ is divided into a parameter of interest $\mu$, usually corresponds to the signal strength and nuisance parameters $\boldsymbol{\Theta}$ that add degrees of

freedom to the model. For a single signal and background contribution counted with a histogram in some observable the expected counts per bin can be expressed in terms of the expected signal $s_i(\boldsymbol{\Theta})$ and background $b_i(\boldsymbol{\Theta})$ in bin $i$, both dependent on the nuisance parameters. The expected count per bin of the observable $n_i$ can then be expressed as

$$\langle n_i \rangle = \mu s_i(\boldsymbol{\Theta}) + b_i(\boldsymbol{\Theta}). \tag{3.1.1}$$

Given that events occur at a constant rate and independently in time, each bin follows a Poisson distribution:

$$P(r, k) = \frac{r^k e^{-r}}{k!}, \tag{3.1.2}$$

where $r$ is the expected rate of occurrences (the prediction) and $k$ is the observed occurrences. A likelihood can then be constructed from a product of the Poisson probabilities and additional terms $c_k$ that help in constraining the model

$$L(\mu, \boldsymbol{\Theta}) = \prod_{j=1}^{N} \frac{(\mu s_j(\boldsymbol{\Theta}) + b_j(\boldsymbol{\Theta}))^{n_j}}{n_j!} e^{-(\mu s_j(\boldsymbol{\Theta}) + b_j(\boldsymbol{\Theta}))} \prod_{k=1}^{M} c_k(\boldsymbol{\Theta}). \tag{3.1.3}$$

These constraint terms can be interpreted as penalties on the likelihood, incorporating prior knowledge into the model. For instance, they can represent another Poisson measurement where only the background is expected, or be used to account for uncertainties, as discussed in detail in Section 3.4.

To test a hypothesized value of $\mu$, the best choice according to the Neyman-Pearson lemma, is the profile likelihood ratio. This ratio reduces the dependence of the likelihood function to the parameter of interest:

$$\lambda(\mu) = \frac{L(\mu, \hat{\hat{\boldsymbol{\Theta}}})}{L(\hat{\mu}, \hat{\boldsymbol{\Theta}})}. \tag{3.1.4}$$

Here, the denominator is the unconditional maximum likelihood estimate, allowing both $\hat{\mu}$ and $\hat{\boldsymbol{\Theta}}$ to vary freely to maximize $L$. The numerator is the maximum likelihood conditioned on some chosen $\mu$ and the set of nuisance parameters $\hat{\hat{\boldsymbol{\Theta}}}$ that maximize the likelihood for that particular $\mu$. This definition gives $0 \leq \lambda \leq 1$

where $\lambda = 1$ corresponds to perfect agreement of the hypothesized value of $\mu$ with the model.

## 3.2 Test Statistic and p-value

To test for a given hypothesis a test statistic serves a quantity that reduces the data set to one value on which the hypothesis is conducted. The test statistic here is a transform of the profile likelihood

$$t(\mu) = -2 \ln \lambda(\mu). \tag{3.2.1}$$

This translates to $t \to 0$ as increasing agreement and $t \to \infty$ as decreasing agreement to the model. A right-tail p-value can then be calculated from the probability density of the test statistic $f(t|\mu)$ as

$$p = \int_{t_{\text{obs}}}^{\infty} f(t|\mu) \mathrm{d}t \tag{3.2.2}$$

Here, $t_{\text{obs}}$ is the test statistic $t$ computed using the particular $\mu$ and observed data. The probability density function $f(t|\mu)$ of the test statistic $t$ quantifies how probable a particular value of $t$ is under a fixed value of the signal strength $\mu$, essentially measuring how frequently a particular value of $t$ occurs in comparison to all other possible values.

The specific form of the test statistic is useful due to existing approximations for $f(t|\mu')$ with $\mu'$ as the true strength parameter [32]. Wald [34] demonstrated that for a single parameter of interest, the test statistic asymptotically approaches a squared distance between the tested parameter $\mu$ and its maximum likelihood estimate $\hat{\mu}$

$$t(\mu) = -2 \ln \lambda(\mu) = \left( \frac{\mu - \hat{\mu}}{\sigma_{\hat{\mu}}} \right)^2 + \mathcal{O}(\frac{1}{\sqrt{N}}), \tag{3.2.3}$$

where $\hat{\mu}$ is normally distributed around its true value $\mu'$ with standard deviation $\sigma_{\hat{\mu}}$. $\hat{\mu}$ is determined by the maximum likelihood fit and the standard deviation is taken from the covariance matrix of the maximum likelihood estimates of the nuisance parameters $V_{ij}(\hat{\boldsymbol{\Theta}})$, detailed in 3.5.

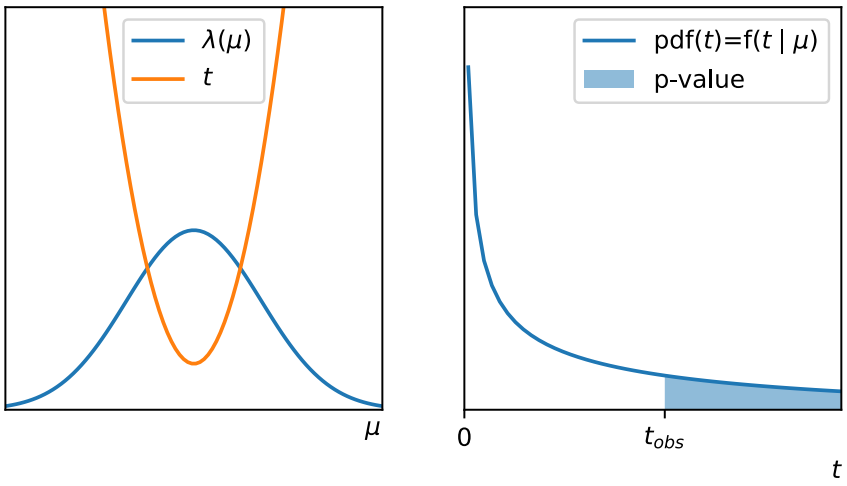


**Figure 3.1:** A sketch to follow the steps to calculate p-values. (**left**) The profile likelihood (／) has essentially some hill-like form with a maximum at $\lambda(\hat{\mu}, \hat{\mathbf{\Theta}})$. The test statistic $t$ (／) is calculated as $-2\ln(\lambda)$. (**right**) For one parameter of interest in the large sample limit $f(t|\mu)$ from equation 3.2.4 follows a non-central chi-squared distribution with one degree of freedom. The blue shaded area under the probability density functions is a right hand sided p-value.

With this result, it can be shown that if $\hat{\mu}$ is Gaussian distributed, the probability density function of $t$ follows a *non-central* $\chi^2$ *distribution* in the large sample limit

$$f(t|\mu) = \frac{1}{2\sqrt{t}} \frac{1}{\sqrt{2\pi}} \left[ \exp\left( -\frac{1}{2} \left( \sqrt{t} + \sqrt{\Lambda_\mu} \right) \right) + \exp\left( -\frac{1}{2} \left( \sqrt{t} - \sqrt{\Lambda_\mu} \right) \right) \right], \quad (3.2.4)$$

with non-centrality parameter

$$\Lambda_\mu = \frac{(\mu - \mu')^2}{\sigma^2}. \quad (3.2.5)$$

Figure 3.1 illustrates these steps. $\Lambda_\mu$ is estimated by setting the observed values to the predicted ones, such that the true value $\mu'$ in $\Lambda_\mu$ becomes the maximum likelihood estimate one $\hat{\mu}$. which results. The dataset that achieves this, with observed event counts per bin exactly matching the predicted ones, is referred to as the 'Asimov' dataset.

The ability to compute p-values allows scientists to state the likelihood that the proposed hypothesis is supported by the observed data. Specifically, the p-value indicates the probability of obtaining data at least as extreme as the observed data if the experiment were repeated many times. This measure reflects the degree of incompatibility between prediction and observation.

In the scientific community, a p-value of 0.05 is commonly accepted as significant. However, particle physicists usually transform the p-value into a significance using the inverse cumulative distribution function of the standard normal distribution:

$$Z = \Phi^{-1}(1 - p). \tag{3.2.6}$$

Thus, the p-value is expressed in terms of the number of standard deviations if the test statistic were normally distributed. The found p-value is thus expressed in terms of the number of standard deviations this p-value would have if the test statistic were standard normal distributed. Particle physicists claim discovery of a new phenomenon for $Z > 5$ ($p < 2.87 \times 10^{-7}$) and exclude hypotheses for $Z > 2$ ($p < 0.05$). The Asimov significance, an estimate for the significance, can be calculated from the counts per bin when setting observed data points to the expected number of events predicted by the model:

$$Z_A = \sqrt{2 \sum_{i \in bins} ((s_i + b_i)(\log(1 + s_i/b_i)) - s_i)}. \tag{3.2.7}$$

A key consideration is that $t$ can assume negative values for $\mu$ which might be non-physical depending on the context. This is managed by cutting off the test statistic for undesired behavior. For instance, an adjusted test statistic for setting upper limits is:

$$q_\mu = \begin{cases} -2 \ln \lambda(\mu) & \hat{\mu} \leq \mu \\ 0 & \hat{\mu} > \mu \end{cases}. \tag{3.2.8}$$

Here, if a tested signal strength $\mu$ is not larger than the maximum estimate, it is not regarded as less compatible and is set to zero. Various cases and approximations of probability density functions in different scenarios are detailed in [32].

## 3.3 The $CL_s$ Value

Particle physicists typically concentrate on two key aspects when performing statistical tests to discover new phenomena: the accurate modeling of known backgrounds and whether there is evidence in the observations for a new phenomenon. This involves assessing two distinct hypotheses: a background only ($b$) and one that involves signal and background ($s + b$). Each will result in a p-value of their own.

To combine these two aspects into a unified metric particle physicists developed the $CL_s$ quantity. This measure not only considers the potential presence of new phenomena but also the accuracy of the background modeling.

$$\mathrm{CL}_s = \frac{p_{s+b}}{1 - p_b} = \frac{\int_{t_{\mathrm{obs}}}^{\infty} f(t_{s+b}|\mu)\mathrm{d}t}{1 - \int_{t_{\mathrm{obs}}}^{\infty} f(t_b|\mu)\mathrm{d}t}. \tag{3.3.1}$$

The numerator represents the p-value for the alternative hypothesis while the denominator penalizes the $p_{s+b}$ based on the compatibility of the background model with observed data. For example, $p_b = 0$ indicates a perfect modeling of backgrounds. This becomes particularly useful in searches with poor sensitivity as the hypothesis test depends crucially on the background estimate. When for instance the background is underestimated, the background only $p_b$-value would be large and would penalize $p_{s+b}$. The concept can also be understood visually from the first figure of the paper that introduced the $CL_s$ quantity [35] as explained in figure 3.2.

## 3.4 HistFactory

A widely-used model in ATLAS for constructing likelihoods, as discussed in section 3.1 is known as HistFactory [36]. It simplifies building a likelihood by breaking it down into fundamental components and considering different categories of model parameters $\boldsymbol{\phi}$.

$$L(\boldsymbol{x}|\boldsymbol{\phi}) = L(\boldsymbol{x}|\overbrace{\boldsymbol{\psi}}^{\text{parameters of interest}}, \underbrace{\boldsymbol{\theta}}_{\text{nuisance parameters}}) = L(\boldsymbol{x}|\overbrace{\boldsymbol{\eta}}^{\text{free}}, \underbrace{\boldsymbol{\chi}}_{\text{constrained}}), \tag{3.4.1}$$

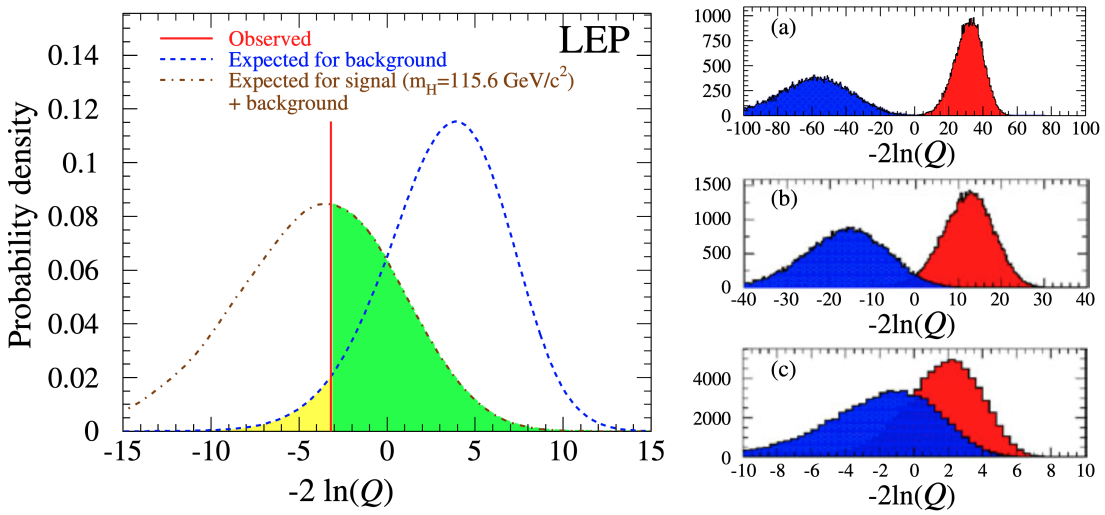


**Figure 3.2:** Probability density functions of test statistics from a Higgs search at LEP, illustrating p-value calculations ($\lambda$ from the full text becomes $Q$). (**left**) The probability density functions of the test statistic $f(t|\mu)$ of the signal + background (／) and background only (／) hypotheses. The p-value is calculated by integration from $t_{\text{obs}}$ (the red observed line (／)) to infinity (see eq. 3.2.2). The green shaded area (■) corresponds to $p_{s+b}$ whereas the yellow area (■) corresponds to $1 - p_b$ since $\int \text{pdf} = 1$. (**right**) Degradation of search sensitivity from (a) to (c). Note the color change in probability density functions: signal + background (■) and background only (■).For example given an observation of ($t_{\text{obs}} \approx 0$), yields for plot (a) $p_b \approx 1$ and $p_{s+b} \approx 0$ resulting in a $\text{CL}_s \approx 0$; with increasing overlap the $\text{CL}_s$ value increases and the sensitivity decreases. Adopted from [35].

HistFactory distinguishes between free parameters $\boldsymbol{\eta}$ and constrained parameters $\boldsymbol{\chi}$, which are used to implement uncertainties into the likelihood. There may be several histograms of an observable, measured in orthogonal kinematic regions, called channels $c$, with bins indexed by $b$. Constraint terms are denoted by $c_\chi$. The likelihood is described as:

$$L(\boldsymbol{n}, \boldsymbol{a} \,|\, \boldsymbol{\eta}, \boldsymbol{\chi}) = \underbrace{\prod_{c \in \text{ channels}} \prod_{b \in \text{ bins}_c} \text{Pois}( \overbrace{n_{cb}}^{\text{observed}} \mid \overbrace{\nu_{cb}\left(\boldsymbol{\eta}, \boldsymbol{\chi}\right)}^{\text{predicted}} )}_{\substack{\text{Simultaneous measurement} \\ \text{of multiple channels}}} \underbrace{\prod_{\chi \in \boldsymbol{\chi}} c_\chi(a_\chi | \, \chi)}_{\substack{\text{constraint terms} \\ \text{for auxiliary measurements}}} \quad . \tag{3.4.2}$$

Here, $\boldsymbol{n}$ represents observed and $\boldsymbol{a}$ auxiliary measurement histograms. The $n_{cb}$ enter the Poisson term per bin and channel, and the predicted counts per bin are governed by the free and constrained parameters $\nu_{cb}(\boldsymbol{\eta}, \boldsymbol{\chi})$. Functions $c_\chi(a_\chi|, \chi)$ penalize the likelihood $L$ with uncertainties $a_\chi$ to constrain the parameter $\chi$, as discussed in detail in section 3.4.1.

### 3.4.1 Modifiers

The prediction is a sum of nominal counts per bin $\nu^0_{scb}$ over all samples $s$ (e.g., $t\bar{t}$, multijet-background, etc.). These nominal counts per bin are subject to uncertainties and have some degree of freedom. This modification to the likelihood is taken into account via the constraint terms, which penalize the likelihood proportional to the modification. There are multiplicative $\kappa_{scb}$ and additive modifiers $\Delta_{scb}$ to the nominal bin count $\nu^0_{scb}$:

$$\nu_{cb}\left(\boldsymbol{\eta}, \boldsymbol{\chi}\right) = \sum_{s \in \text{ samples}} \nu_{scb}\left(\boldsymbol{\eta}, \boldsymbol{\chi}\right) \tag{3.4.3}$$

$$= \sum_{s \in \text{ samples}} \underbrace{\left( \prod_{\kappa \in \boldsymbol{\kappa}} \kappa_{scb}\left(\boldsymbol{\eta}, \boldsymbol{\chi}\right) \right)}_{\text{multiplicative modifiers}} \nu^0_{scb} + \underbrace{\sum_{\Delta \in \boldsymbol{\Delta}} \Delta_{scb}\left(\boldsymbol{\eta}, \boldsymbol{\chi}\right)}_{\text{additive modifiers}} . \tag{3.4.4}$$

Considering one nuisance parameter $\chi$ controlling a multiplicative modifier $\kappa_{scb}(\chi)$ on $\nu^0_{scb}$, an optimum can be found by modifying the prediction to move closer to

the observed value while keeping the constraint term controlled by the same $\chi$ at values where the penalization of the likelihood remains insignificant.

Histfactory implements various types of modifiers detailed in [36–38]. The ones used in this work include a free rate modifier for the signal strength $\mu$ that affects all bins equally:

$$\nu_{scb}(\mu) = \mu\nu^0_{scb}, \tag{3.4.5}$$

and inter-/extrapolation functions $I(\alpha)$ depending on a nuisance parameter $\alpha$ that continuously scale the nominal counts per bin for a given uncertainty. The modifiers control the nominal bin count $\nu_{scb}$ such that $\alpha = \pm 1$ results in to 1 standard deviation uncertainties:

$$I(\alpha = \pm 1)\nu^0_{scb} = \nu^{\pm}_{scb}. \tag{3.4.6}$$

These modifications are accompanied by a Gaussian constraint term to the likelihood:

$$\text{Gaus}(\mu|x, \sigma) = \frac{1}{\sigma\sqrt{2\pi}} e^{-\frac{1}{2}\left(\frac{x-\mu}{\sigma}\right)^2}. \tag{3.4.7}$$

This constraint term is scaled to one standard deviation $\sigma$ controlled by the nuisance parameter $\alpha$: $\text{Gauss}(\mu = 0|\alpha, \sigma = 1)$. HistFactory offers several implementations for $I(\alpha)$. This thesis uses the recommended modifiers for normalization uncertainties NormSys and shape uncertainties HistoSys, employed by the cabinetry fitting framework [39].

### Normalization Inter-/Extrapolation

Normalization uncertainties (NormSys) are implemented via a six-term polynomial interpolation and exponential extrapolation function as a multiplicative modifier ($\kappa_{scb}$ in equation in equation 3.4.4) on the nominal rate:

$$\nu_{scb}(\alpha) = \nu^0_{scb} I_{\text{poly|exp.}}(\alpha; \nu^0_{scb}, \nu^+_{scb}, \nu^-_{scb}, 1) \tag{3.4.8}$$

with nuisance parameter $\alpha$, nominal bin rate $\nu^0_{scb}$, one standard upward and downward deviations $\nu^{\pm}_{scb}$, and $\alpha_0$ defining the crossover between the polynomial

and exponential function:

$$I_{\text{poly|exp.}}(\alpha; I^0, I^+, I^-, \alpha_0) = \begin{cases} \left(\frac{I^+}{I^0}\right)^{\alpha} & \alpha \geq \alpha_0 \\ 1 + \sum_{i=1}^{6} a_i \alpha^i & |\alpha| < \alpha_0 \\ \left(\frac{I^-}{I^0}\right)^{-\alpha} & \alpha < -\alpha_0 \end{cases} \tag{3.4.9}$$

The $a_i$ are fixed through the boundary conditions

$$\nu_{scb}(\alpha = \pm\alpha_0), \left.\frac{\mathrm{d}\nu_{scb}}{\mathrm{d}\alpha}\right|_{\alpha=\pm\alpha_0}, \text{and } \left.\frac{\mathrm{d}^2\nu_{scb}}{\mathrm{d}\alpha^2}\right|_{\alpha=\pm\alpha_0}. \tag{3.4.10}$$

A single nuisance parameter $\alpha$ controls all the bins of one normalization systematic simultaneously in a shape preserving manner.

#### Correlated Shape Inter-/Extrapolation

The most common histogram uncertainty HistoSys scales the uncertainties $\nu_{sb}^{+}$ with a linear inter- and extrapolation

$$\nu_{scb}(\alpha) = \nu_{scb}^{0}(\alpha) + I_{\text{lin.}}(\alpha; \nu_{scb}^{0}, \nu_{sb}^{+}, \nu_{sb}^{-}) \tag{3.4.11}$$

with

$$I_{\text{lin.}}(\alpha; I^0, I^+, I^-) = \begin{cases} \alpha(I^+ - I^0) & \alpha \geq 0 \\ \alpha(I^0 - I^-) & \alpha < 0 \end{cases} \tag{3.4.12}$$

### 3.4.2 Shape Uncertainty Recommendation

In this analysis, all shape uncertainties are always applied with an additional normalization uncertainty. The reason is that the linear extrapolation of the shape uncertainty can yield negative bin count values, particularly with the standard setting of the maximum likelihood fit, which probes nuisance parameters for $\pm 5\sigma$. When augmented with a normalization uncertainty modifier that uses exponential interpolation, the uncertainty is protected against negative yields, as shown in figure 3.3.

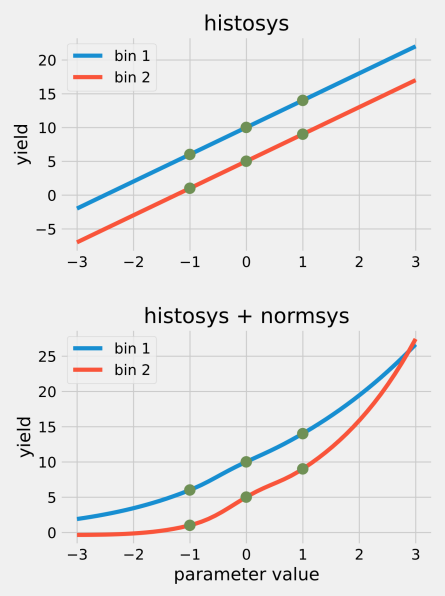


**Figure 3.3:** Effect of nuisance parameter pulling on histogram yields with and without applying an additional normalization uncertainty to a HistoSys shape uncertainty. Adopted from [40].

## 3.5 Uncertainty Extraction

The standard error of a quantity is determined by measuring the square root of its variance. The covariance matrix is a generalization of variance for two random variables $X_i, X_j$

$$V_{ij} = \mathrm{Cov}(X_i, X_j) = \mathrm{E}[(X_i - \mathrm{E}[X_i])(X_j - \mathrm{E}[X_j])]. \tag{3.5.1}$$

In the context of maximum likelihood estimation, the covariance matrix of the nuisance parameters $\boldsymbol{\theta}$ can be approximated in the large sample limit by the inverse of the negative Hessian of the log-likelihood function $L$

$$V_{ij} = \left[ -\frac{\partial^2 L(\boldsymbol{\theta})}{\partial\theta_i \partial\theta_j} \right]^{-1}. \tag{3.5.2}$$

The covariance matrix holds the variances and thus the uncertainties of the nuisance parameters along its diagonal, and the covariances between components off-diagonal. When propagating uncertainties, these covariances contribute to the

overall uncertainty. This can be illustrated by examining the variance of a function $f(\theta_1, \theta_2)$ that depends on two parameters with individual $\sigma_1, \sigma_2$ uncertainties

$$\mathrm{Var}(f(\theta_1, \theta_2)) = \left(\frac{\partial f}{\partial \theta_1}\right)^2 \sigma_1^2 + \left(\frac{\partial f}{\partial \theta_2}\right)^2 \sigma_2^2 + 2\left(\frac{\partial f}{\partial \theta_1}\right)\left(\frac{\partial f}{\partial \theta_2}\right)\sigma_{12}. \tag{3.5.3}$$

If the parameters $\theta_1$ and $\theta_2$ are correlated the cross-term $2\left(\frac{\partial f}{\partial \theta_1}\right)\left(\frac{\partial f}{\partial \theta_2}\right)\sigma_{12}$ contributes to the overall uncertainty. Consequently, large correlations between parameters, indicated by significant off-diagonal terms, are disadvantageous for constraining the model.

# Bibliography

[1] M. Grazzini, G. Heinrich, S. Jones, S. Kallweit, M. Kerner, J. M. Lindert, and J. Mazzitelli. Higgs boson pair production at NNLO with top quark mass effects. *Journal of High Energy Physics*, 2018(5), may 2018. doi:10.1007/jhep05(2018)059. URL `https://doi.org/10.1007%2Fjhep05%282018%29059`.

[2] Frédéric A. Dreyer and Alexander Karlberg. Vector-boson fusion higgs pair production at $n^3LO$. *Phys. Rev. D*, 98:114016, Dec 2018. doi:10.1103/PhysRevD.98.114016.

[3] Daniel de Florian, D Fontes, J Quevillon, M Schumacher, FJ Llanes-Estrada, AV Gritsan, E Vryonidou, A Signer, P de Castro Manzano, D Pagani, et al. *arXiv: Handbook of LHC Higgs Cross Sections: 4. Deciphering the Nature of the Higgs Sector*. Number arXiv: 1610.07922. Cern, 2016.

[4] ATLAS Collaboration. Search for nonresonant pair production of higgs bosons in the b $b^-$ b $b^-$ final state in p p collisions at s= 13 tev with the atlas detector. *Phys. Rev. D*, 108(5):052003, 2023. doi:10.1103/PhysRevD.108.052003.

[5] Dale Charles Abbott, William Keaton Balunas, Lucas Santiago Borgna, Alexander Emerman, James Frost, Sean Joseph Gasiorowski, James Cameron Grundy, Nicole Michelle Hartman, Shota Hayashida, Todd Brian Huffman, Cigdem Issever, Michael Kagan, Yu Nakahama, Santiago Rafael Paredes Saenz, Attilio Picazio, Jana Schaarschmidt, Todd Seiss, Mel Shochet, Beojan Stanislaus, Maximilian J Swiatlowski, Rafael Teixeira De Lima, Stephane Willocq, Anna Goussiou, Nikolaos Konstantinidis, Sau Lan Wu, Chen-Hsun Chan, Chen Zhou, Rui Zhang, Christopher Gubbels, Marta Maja Czurylo, Raif Rafideen Bin Norisam, Teng Jian Khoo, Arely Cortes-Gonzalez, Daniel Guest, Liaoshan Shi, Iza Veliscek, Marco Valente, Alessandra Betti, Christopher Don Milke, and Katharine Leney. Supporting Document: The Search for Resonant HH Production Decaying to the 4b Final State Using the Full Run-2 Data and the Boosted Analysis Channel. Technical report, CERN, Geneva, 2020. URL `https://cds.cern.ch/record/2708599`.

[6] Fady Bishara, Roberto Contino, and Juan Rojo. Higgs pair production in vector-boson fusion at the lhc and beyond. *The European Physical Journal C*, 77:1–26, 2017. doi:10.1140/epjc/s10052-017-5037-9.

[7] Validation of signal Monte Carlo event generation in searches for Higgs boson pairs with the ATLAS detector. Technical report, CERN, Geneva, 2019. URL `https://cds.cern.ch/record/2665057`. All figures including auxiliary figures are available at https://atlas.web.cern.ch/Atlas/GROUPS/PHYSICS/PUBNOTES/ATL-PHYS-PUB-2019-007.

[8] ATLAS Collaboration. Luminosity determination in $pp$ collisions at $\sqrt{s} = 13$ TeV using the ATLAS detector at the LHC. 2022. doi:10.48550/ARXIV.2212.09379.

[9] Johan Alwall, R Frederix, S Frixione, V Hirschi, Fabio Maltoni, Olivier Mattelaer, H-S Shao, T Stelzer, P Torrielli, and M Zaro. The automated computation of tree-level and next-to-leading order differential cross sections, and their matching to parton shower simulations. *Journal of High Energy Physics*, 2014(7):1–157, 2014.

[10] Francis Halzen, A Martin, and Leptons Quarks. An introductory course in modern particle physics. *John and Wiley*, 1984.

[11] Mark Thomson. *Modern particle physics*. Cambridge University Press, 2013.

[12] M. Tanabashi et al. Review of particle physics. *Phys. Rev. D*, 98:030001, Aug 2018. doi:10.1103/PhysRevD.98.030001.

[13] Torbjörn Sjöstrand, Stefan Ask, Jesper R. Christiansen, Richard Corke, Nishita Desai, Philip Ilten, Stephen Mrenna, Stefan Prestel, Christine O. Rasmussen, and Peter Z. Skands. An introduction to PYTHIA 8.2. *Comput. Phys. Commun.*, 191:159, 2015. doi:10.1016/j.cpc.2015.01.024.

[14] Stefan Höche. Introduction to parton-shower event generators. In *Theoretical Advanced Study Institute in Elementary Particle Physics: Journeys Through the Precision Frontier: Amplitudes for Colliders*, pages 235–295, 2015. doi:10.1142/9789814678766_0005.

[15] GEANT4 Collaboration, S. Agostinelli, et al. GEANT4 – a simulation toolkit. *Nucl. Instrum. Meth. A*, 506:250, 2003. doi:10.1016/S0168-9002(03)01368-8.

[16] Frederic Renner. Higgs pair analysis using python. `https://gitlab.cern.ch/frenner/pyhh`, 2024. Accessed: May 27, 2024.

[17] The ATLAS Collaboration. Athena analysis framework. URL `https://gitlab.cern.ch/atlas/athena/`.

[18] Sau Lan Wu, Ashutosh Kotwal, Arely Cortes Gonzalez, Michael Kagan, Shu Li, Maximilian J Swiatlowski, Liaoshan Shi, Janna Katharina Behr, Valentina Cairo, Thomas Andrew Schwarz, Sebastien Rettie, Yanlin Liu, Rui Zhang, Rachel Jordan Hyneman, Sanmay Ganguly, Dilia Maria Portillo Quintero, Kunlin Ran, Marco Valente, Mohamed Belfkir, Rafael Teixeira De Lima, Zhen Wang, Daariimaa Battulga, Jem Aizen Mendiola Guhit, Yuwen Ebony Zhang, Russell Bate, Karl Ver Hage Falb, Salah Nasri, Hemza Azri, and Marcus Vinicius Gonzalez Rodrigues. Search for resonant and non-resonant boosted Higgs boson pair production in *bbbb* final state via vector-boson-fusion (VBF) production using the full Run 2 data with ATLAS detector. Technical report, CERN, Geneva, 2023. URL `https://cds.cern.ch/record/2848140`.

[19] Michael Rauch. Vector-boson fusion and vector-boson scattering, 2016.

[20] Will Buttinger. Background estimation with the abcd method. URL `https://twiki.cern.ch/twiki/pub/Main/ABCDMethod/ABCDGuide_draft18Oct18.pdf`. Last accessed: 2023-11-21.

[21] Gregor Kasieczka, Benjamin Nachman, Matthew D. Schwartz, and David Shih. Automating the abcd method with machine learning. *Phys. Rev. D*, 103:035021, Feb 2021. doi:10.1103/PhysRevD.103.035021. URL `https://link.aps.org/doi/10.1103/PhysRevD.103.035021`.

[22] Constraints on the Higgs boson self-coupling from the combination of single-Higgs and double-Higgs production analyses performed with the ATLAS experiment. Technical report, CERN, Geneva, 2019. URL `http://cds.cern.ch/record/2693958`. All figures including auxiliary figures are available at https://atlas.web.cern.ch/Atlas/GROUPS/PHYSICS/CONFNOTES/ATLAS-CONF-2019-049.

[23] ATLAS Collaboration atlas. publications@ cern. ch, Georges Aad, B Abbott, DC Abbott, A Abed Abud, K Abeling, DK Abhayasinghe, SH Abidi, OS AbouZeid, NL Abraham, et al. Jet energy scale and resolution measured in proton–proton collisions at s= 13 tev with the atlas detector. *The European Physical Journal C*, 81(8):689, 2021. doi:10.48550/arXiv.2007.02645.

[24] The ATLAS collaboration. In situ calibration of large-radius jet energy and mass in 13 tev proton–proton collisions with the atlas detector. *The European Physical Journal C*, 79(2):135, 2019. doi:10.1140/epjc/s10052-019-6632-8. URL `https://doi.org/10.1140/epjc/s10052-019-6632-8`.

[25] ATLAS Collaboration. Measurement of the ATLAS Detector Jet Mass Response using Forward Folding with $80\,\text{fb}^{-1}$ of $\sqrt{s} = 13\,\text{TeV}$ $pp$ data. ATLAS-CONF-2020-022, 2020. URL `https://cds.cern.ch/record/2724442`.

[26] Identification of Boosted Higgs Bosons Decaying Into $b\bar{b}$ With Neural Networks and Variable Radius Subjets in ATLAS. Technical report, CERN, Geneva, 2020. URL `https://cds.cern.ch/record/2724739`. All figures including auxiliary figures are available at https://atlas.web.cern.ch/Atlas/GROUPS/PHYSICS/PUBNOTES/ATL-PHYS-PUB-2020-019.

[27] ATLAS Collaboration. Efficiency corrections for a tagger for boosted $H \to b\bar{b}$ decays in $pp$ collisions at $\sqrt{s} = 13$ TeV with the ATLAS detector. Technical report, CERN, Geneva, 2021. URL `https://cds.cern.ch/record/2777811`.

[28] The ATLAS collaboration. Particle Modeling Group systematic uncertainty recipes. URL `https://twiki.cern.ch/twiki/bin/view/AtlasProtected/PmgSystematicUncertaintyRecipes`. Last accessed: 2023-11-29.

[29] Jon Butterworth, Stefano Carrazza, Amanda Cooper-Sarkar, Albert De Roeck, Joël Feltesse, Stefano Forte, Jun Gao, Sasha Glazov, Joey Huston, Zahari Kassabov, Ronan McNulty, Andreas Morsch, Pavel Nadolsky, Voica Radescu, Juan Rojo, and Robert Thorne. Pdf4lhc recommendations for lhc run ii. *Journal of Physics G: Nuclear and Particle Physics*, 43(2):023001, January 2016. ISSN 1361-6471. doi:10.1088/0954-3899/43/2/023001. URL `http://dx.doi.org/10.1088/0954-3899/43/2/023001`.

[30] Lukas Heinrich, Matthew Feickert, and Giordon Stark. pyhf: v0.7.2. URL `https://doi.org/10.5281/zenodo.1169739`. https://github.com/scikit-hep/pyhf/releases/tag/v0.7.2.

[31] Lukas Heinrich, Matthew Feickert, Giordon Stark, and Kyle Cranmer. pyhf: pure-python implementation of histfactory statistical models. *Journal of Open Source Software*, 6(58):2823, 2021. doi:10.21105/joss.02823. URL `https://doi.org/10.21105/joss.02823`.

[32] Glen Cowan, Kyle Cranmer, Eilam Gross, and Ofer Vitells. Asymptotic formulae for likelihood-based tests of new physics. *The European Physical Journal C*, 71:1–19, 2011.

[33] Olaf Behnke, Kevin Kröninger, Grégory Schott, and Thomas Schörner-Sadenius. *Data analysis in high energy physics: a practical guide to statistical methods*. John Wiley & Sons, 2013.

[34] Abraham Wald. Tests of statistical hypotheses concerning several parameters when the number of observations is large. *Transactions of the American Mathematical society*, 54(3):426–482, 1943.

[35] Alexander L Read. Presentation of search results: the cls technique. *Journal of Physics G: Nuclear and Particle Physics*, 28(10):2693, 2002.

[36] Kyle Cranmer, George Lewis, Lorenzo Moneta, Akira Shibata, and Wouter Verkerke. HistFactory: A tool for creating statistical models for use with RooFit and RooStats. Technical report, New York U., New York, 2012. URL `https://cds.cern.ch/record/1456844`.

[37] Lukas Heinrich. Introduction to model building within pyhf. `https://pyhf.readthedocs.io/en/v0.7.2/intro.html`, 2021. [Online; accessed 27-June-2023].

[38] Lukas Heinrich. *Searches for Supersymmetry, RECAST, and Contributions to Computational High Energy Physics*. PhD thesis, New York University, 2019.

[39] *Building and steering template fits with cabinetry*, March 2021. Zenodo. doi:10.5281/zenodo.4627038. URL `https://doi.org/10.5281/zenodo.4627038`.

[40] Alexander Held. Introduction to statistics. `https://indico.cern.ch/event/1237730/contributions/5297885/`, 2023. [Online; accessed 04-July-2024].

**Statutory Declaration - Eidesstattliche Erklärung**

I declare that I have authored this thesis independently, that I have not used other than the declared sources/ resources and that I have explicitly marked all materials which has been quoted either literally or by content from the used sources.

Hiermit erkläre ich, dass ich die vorliegende Arbeit selbstständig verfasst, andere als die angegebenen Quellen/Hilfsmittel nicht benutzt und die den benutzten Quellen wörtlich und inhaltlich entnommenen Stellen als solche kenntlich gemacht habe.

Berlin, 12.07.2024

Frederic Renner